Unit cells for the simulation of hexagonal ice

J. A. Hayward and J. R. Reimers

Citation: The Journal of Chemical Physics **106**, 1518 (1997); doi: 10.1063/1.473300
View online: http://dx.doi.org/10.1063/1.473300
View Table of Contents: http://scitation.aip.org/content/aip/journal/jcp/106/4?ver=pdfcov
Published by the AIP Publishing

Unit cells for the simulation of hexagonal ice

J. A. Hayward and J. R. Reimers
School of Chemistry, University of Sydney, New South Wales 2006 Australia

(Received 1 July 1996; accepted 10 October 1996)

A number of periodic lattices have historically been used to represent ice-1h in computer simulations. These vary in size, shape, and method of generation, and while they have served their intended purposes, their properties have rarely been documented in detail and their intercompatibility is unknown. We develop a method for generating sets of internally consistent lattices and apply it to determine eight unit cells containing from 96 to 768 water molecules in both near-cubic and slab arrangements. It can easily be applied to generate additional (larger) cells or representations of specific crystal faces. Each unit cell in this set has zero net dipole moment and minimal net quadrupole moment and is optimized using four different criteria to measure the randomness of the hydrogen bonding; if required, these criteria can easily be modified to suit the intended application and alternate sets thus generated. We find that Cota and Hoover's much used constraint for selecting unit cells with zero dipole moment is too restrictive, not permitting a fully random hydrogen-bonding network; also, unit-cell generation methods based on potential-energy minimization are found to prefer unrepresentative, highly ordered structures. © *1997 American Institute of Physics.* [S0021-9606(97)51003-8]

I. INTRODUCTION

Computer simulations of ice-1h are of considerable general interest, with some recent prominent applications being to the properties of ice surfaces including melting and freezing phenomena.[1–4] The basic properties of ice-1h were determined by Bernal and Fowler:[5,6] it comprises two intersecting hexagonal oxygen-atom lattices, with a continuous network of randomly oriented hydrogen bonds. Key features were elucidated by Rahman and Stillinger,[7] who also performed the first computer simulations of ice using a Monte Carlo method. Modern computer simulations typically involve the use of a large unit cell to describe the crystal, its dimensions being sufficiently large that the internal hydrogen-bonding pattern is random.

For most unit-cell-based applications, it is desired that as many as possible of the electric multipole moments of the charge distribution within the unit cell be zero in order to minimize long-range interactions between unit cells,[7] and a method for the generation of structures constrained to have zero dipole moment was developed by Cota and Hoover.[8] This method has been adapted by others (see, e.g., Refs. 3, 9 and 10) in order to generate unit cells of various sizes and shapes. In particular, Cota and Hoover generated two unit cells containing 48 and 96 water molecules: they claimed that, in addition to zero dipole moment, these unit cells also displayed zero quadrupole and octupole moments. Following suggestions by Haymet,[11] we find that this is not obviously so, and in fact we are unable to find *any* existing model ice-1h unit cell which (in any representation) actually has zero quadrupole moment. Also, while claims have been made that the hydrogen bonding in various ice-1h lattices is random, this has not been documented. Last, while lattices spanning a range of sizes are available, these have not been generated in an internally consistent manner and there is no guarantee that similar results for non-size-dependent properties would be obtained from the available lattices. These facts have prompted us to reinvestigate methods for generating ice-1h lattices, presenting a method for producing consistent, random lattices with ''small'' multipole moments for arbitrary lattice shapes and sizes.

We consider basic properties of ice-1h unit cells (including nonuniqueness of the multipole moments) in Sec. II and the criteria used to select optimal unit-cell structures in Sec. III, describe the basic computational procedure in Sec. IV, present results for small clusters and lattices in Sec. V, and the main results in Sec. VI, and describe long-range summations of the lattice energies in Sec. VII. Throughout, results are obtained for classical, rigid water molecules at 0 K. Our results and methods may readily by applied in more sophisticated calculations which allow for intermolecular and intramolecular vibrations, finite temperature, and quantum effects such as proton tunneling and zero-point motion (see, e.g., Ref. 12).

II. BASIC LATTICE PROPERTIES

In ice-1h, the oxygen atoms lie on two intersecting hexagonal lattices. When the hydrogen atoms are also considered, a minimum of four water molecules are required per unit cell. At each of these four different sites, the orientation of water hydrogen atoms can be selected from a (mutually exclusive) set of 6 possibilities so that a total of 24 unique water orientations exist. Each of the arrangements for each site is listed in Table I in terms of orthogonal unit vectors representing the molecular symmetry (**a**) and in-plane (**b**) axes. From them the displacements $\mathbf{R_1}$ and $\mathbf{R_2}$ of the actual hydrogen atoms can be obtained given the O–H bond length R_{OH} and $\measuredangle$HOH θ using

$$\mathbf{R_1} = R_{\mathrm{OH}} \cos\frac{\theta}{2}\mathbf{a} + R_{\mathrm{OH}} \sin\frac{\theta}{2}\mathbf{b},$$

 0021-9606/97/106(4)/1518/12/$10.00

TABLE I. Unit vectors **a** (symmetry axis) and **b** (in-plane) describing all six possible water orientations at each of the four crystal sites.

Site	Orient.	a_x	a_y	a_z	b_x	b_y	b_z
1	1	0	$(2/3)^{1/2}$	$(1/3)^{1/2}$	-1	0	0
	2	$-(1/2)^{1/2}$	$-(1/6)^{1/2}$	$(1/3)^{1/2}$	$-1/2$	$(3/4)^{1/2}$	0
	3	$-(1/2)^{1/2}$	$(1/6)^{1/2}$	$-(1/3)^{1/2}$	$1/2$	$-(1/12)^{1/2}$	$-(2/3)^{1/2}$
	4	$(1/2)^{1/2}$	$-(1/6)^{1/2}$	$(1/3)^{1/2}$	$-1/2$	$-(3/4)^{1/2}$	0
	5	$(1/2)^{1/2}$	$(1/6)^{1/2}$	$-(1/3)^{1/2}$	$-1/2$	$-(1/12)^{1/2}$	$-(2/3)^{1/2}$
	6	0	$-(2/3)^{1/2}$	$-(1/3)^{1/2}$	0	$(1/3)^{1/2}$	$-(2/3)^{1/2}$
2	1	$(1/2)^{1/2}$	$(1/6)^{1/2}$	$-(1/3)^{1/2}$	$1/2$	$-(3/4)^{1/2}$	0
	2	0	$-(2/3)^{1/2}$	$-(1/3)^{1/2}$	-1	0	0
	3	$(1/2)^{1/2}$	$-(1/6)^{1/2}$	$(1/3)^{1/2}$	$-1/2$	$(1/12)^{1/2}$	$(2/3)^{1/2}$
	4	$-(1/2)^{1/2}$	$(1/6)^{1/2}$	$-(1/3)^{1/2}$	$-1/2$	$-(3/4)^{1/2}$	0
	5	0	$(2/3)^{1/2}$	$(1/3)^{1/2}$	0	$-(1/3)^{1/2}$	$(2/3)^{1/2}$
	6	$-(1/2)^{1/2}$	$-(1/6)^{1/2}$	$(1/3)^{1/2}$	$1/2$	$(1/12)^{1/2}$	$(2/3)^{1/2}$
3	1	0	$(2/3)^{1/2}$	$-(1/3)^{1/2}$	-1	0	0
	2	$-(1/2)^{1/2}$	$-(1/6)^{1/2}$	$-(1/3)^{1/2}$	$-1/2$	$(3/4)^{1/2}$	0
	3	$-(1/2)^{1/2}$	$(1/6)^{1/2}$	$(1/3)^{1/2}$	$1/2$	$-(1/12)^{1/2}$	$(2/3)^{1/2}$
	4	$(1/2)^{1/2}$	$-(1/6)^{1/2}$	$-(1/3)^{1/2}$	$-1/2$	$-(3/4)^{1/2}$	0
	5	$(1/2)^{1/2}$	$(1/6)^{1/2}$	$(1/3)^{1/2}$	$-1/2$	$-(1/12)^{1/2}$	$(2/3)^{1/2}$
	6	0	$-(2/3)^{1/2}$	$(1/3)^{1/2}$	0	$(1/3)^{1/2}$	$(2/3)^{1/2}$
4	1	$(1/2)^{1/2}$	$(1/6)^{1/2}$	$(1/3)^{1/2}$	$1/2$	$-(3/4)^{1/2}$	0
	2	0	$-(2/3)^{1/2}$	$(1/3)^{1/2}$	-1	0	0
	3	$(1/2)^{1/2}$	$-(1/6)^{1/2}$	$-(1/3)^{1/2}$	$-1/2$	$(1/12)^{1/2}$	$-(2/3)^{1/2}$
	4	$-(1/2)^{1/2}$	$(1/6)^{1/2}$	$(1/3)^{1/2}$	$-1/2$	$-(3/4)^{1/2}$	0
	5	0	$(2/3)^{1/2}$	$-(1/3)^{1/2}$	0	$-(1/3)^{1/2}$	$-(2/3)^{1/2}$
	6	$-(1/2)^{1/2}$	$-(1/6)^{1/2}$	$-(1/3)^{1/2}$	$1/2$	$(1/12)^{1/2}$	$-(2/3)^{1/2}$

$$\mathbf{R_2}=R_{\mathrm{OH}}\cos\frac{\theta}{2}\mathbf{a}-R_{\mathrm{OH}}\sin\frac{\theta}{2}\mathbf{b}. \tag{1}$$

The basic four-molecule unit cell is in itself hexagonal,[5] and any number of these basic units can be included in a larger unit cell allowing for more random hydrogen orientations; properties of some such important small unit cells have been discussed in detail elsewhere (see, e.g., Refs. 2,5, and 13–17). In particular, two of these units may be combined to form an eight-membered unit cell which has overall orthorhombic symmetry. As orthorhombic unit cells are advantageous in computer simulations, we consider this as our basic building block. It has the dimensions

$$x^0_{\prime}=(8/3)^{1/2}R,\quad y^0_{\prime}=8^{1/2}R,\ \text{and}\ z^0_{\prime}=8R/3, \tag{2}$$

where R is the nearest-neighbor O-O separation, and the locations and types of the eight oxygen atoms in this basic cell are listed in Table II. We construct various large unit cells for ice by replicating this building block by translation n_x, n_y, and n_z times in the x,y, and z directions, respectively, producing unit cells labeled $n_x\times n_y\times n_z$ containing a total of $N=8n_xn_yn_z$ water molecules. The unit cell dimensions $x_{\prime}$,$y_{\prime}$, and $z_{\prime}$ are given by

$$x_{\prime}=n_xx^0_{\prime},\quad y_{\prime}=n_yy^0_{\prime},\quad \text{and}\quad z_{\prime}=n_zz^0_{\prime}, \tag{3}$$

while the radius r_{in} of the inscribed sphere of the unit cell is half of the minimum value of these lengths. The number of

TABLE II. Coordinates x,y,z, and site identity of the eight molecules inside the smallest possible orthorhombic unit cell for ice-1h in terms of the cell lengths $x^0_{\prime}$,$y^0_{\prime}$ and $z^0_{\prime}$ as defined in Eq. (2).

Molecule	Site	$4x/x^0_{\prime}$	$6y/y^0_{\prime}$	$16z/z^0_{\prime}$
1	1	1	1	3
2	2	3	2	5
3	3	1	1	13
4	4	3	2	11
5	1	3	4	3
6	2	1	5	5
7	3	3	4	13
8	4	1	5	11

TABLE III. Properties of selected unit cells: N is the number of water molecules contained; H indicates hexagonal symmetry while O indicates orthorhombic; $x_{\prime}$,$y_{\prime}$,$z_{\prime}$ are the cell lengths in Å, while r_{in} is the inscribed-sphere radius in Å, all evaluated at $R=2.76$ Å, and n_{in} is the number of coordination shells inside the inscribed sphere. Various unit cell names (see text) are 3×2×2-CH: Cota and Hoover's (Ref. 8) 96-molecule unit cell; 3×2×2-h: hexagonal lattice; 3×2×2-C2: using constraint C2; 3×2×2-e: lowest energy C2 structure for the RWK2, TIP3P, and SPC/E potentials; and 4×3×2-a: the unit cell of Deutsch *et al.* (Ref. 9).

Cell	Sym.	Constr.	N	$x_{\prime}$	$y_{\prime}$	$z_{\prime}$	r_{in}	n_{in}
3×2×2-CH	H	C2	96	13.52	15.61	14.72	6.76	6
3×2×2-h	H	C1	96	13.52	15.61	14.72	6.76	6
3×2×2-C2	O	C2	96	13.52	15.61	14.72	6.76	6
3×2×2e[b]	O	C2	96	13.52	15.61	14.72	6.76	6
3×2×2	O	C1	96	13.52	15.61	14.72	6.76	6
4×3×2	O	C1	192	18.03	23.42	14.72	7.36	8
4×3×2-a	O	C2	192	18.03	23.42	14.72	7.36	8
5×3×3	O	C1	360	22.54	23.42	22.08	11.04	22
6×3×3	O	C1	432	27.04	23.42	22.08	11.04	22
9×5×1	O	C1	360	40.56	39.03	7.36	3.68[a]	1[a]
6×4×4	O	C1	768	27.04	31.23	29.44	13.52	36

[a]6 shells are actually used in subsequent calculations.
[b]This is actually two units of a smaller 3×2×1 unit cell.

TABLE IV. Hydrogen orientations (see Table I) for the eight water molecules in subcell $c=c_0+c_1=1+i_y+n_y i_x+n_x n_y i_z$, where $i_x=0\rightarrow n_x-1$, $i_y=0\rightarrow n_y-1$, $i_z=0\rightarrow n_z-1$ index the translation of the original subcell specified in Table II.

Unitn Cell	c_0	$c_1=1$	$c_1=2$	$c_1=3$	$c_1=4$	$c_1=5$	$c_1=6$	$c_1=7$	$c_1=8$	$c_1=9$	$c_1=10$	$c_1=11$	$c_1=12$
3×2×2-CH	0	22554235	41131463	64361524	53516314	36222542	51663641	45341436	36644153	24155352	26226341	32266163	15415215
3×2×2-h	0	41431425	34135341	66516136	11431561	11533642	45645352	34555236	64265225	26112514	32364362	26626225	43342514
3×2×2-C2	0	32432463	55223562	43512416	11451634	66516215	41365324	53244235	62132443	45345352	66622661	11263541	11553416
3×2×2-e	0	36226341	26326143	13512435	11533425	45645216	45645216	36226341	26326143	13512435	11533425	45645216	45645216
3×2×2	0	34533562	13626125	24431662	66416216	24535126	15621641	43244215	45345216	53342551	34135125	41363641	22556334
4×3×2	0	13322541	34553514	13516135	41533425	32152651	62532624	62432624	62362641	64533642	55641614	64131463	15411453
	12	11665362	45225226	26624126	41363542	32454352	24455334	51265263	43246135	15115116	45115334	62152436	36624361
4×3×2-a	0	36626324	45111534	36514136	26622426	32452514	11535342	34451416	53246215	66514153	15325361	62364263	24435125
	12	11435125	53512436	13412436	45645352	64453634	41555216	32156153	36246216	45221561	45321641	22132463	36626324
5×3×3	0	64133642	22454136	13226341	26512453	53224362	66416215	32534263	41433562	36642415	66644136	55641634	26114253
	12	22156136	15225126	34455351	66326143	53244215	64155334	15641651	62154135	34153552	22152551	55321524	11363641
	24	43344253	26414334	62362641	53244115	32556116	51261463	24435126	34665263	62662642	15511552	34261562	55241415
	36	34431561	11365342	26226163	13414136	53224361	24553436	64535324	45513514	32132624			
6×3×3	0	64131662	24431624	62156314	22452552	15645116	53244253	53242435	15345351	64365143	55223662	26226341	26324163
	12	15625226	24433463	36414116	22556334	24533426	11665361	53414334	64555314	64363443	64531524	15323541	32154235
	24	32554136	11431661	41153534	62262524	51555314	41151652	41155216	66224361	66116351	43324163	11435324	22552651
	36	34451634	43516235	41155116	15345334	43516216	62262561	24261562	55621641	66114216	34263542	15625125	36514153
	48	34363443	36622542	32432561	26322425	32536243	41661624						
9×5×1	0	45341435	55115215	62136225	45341534	11551651	22362562	11665143	51453416	36244352	66244351	53112436	53244351
	12	64151453	36246115	34133541	41531662	66226341	26342551	34131463	32432661	64431562	36412453	32262463	32454136
	24	53416216	22554334	22552651	41363624	43324362	45625225	62266324	62132463	51261662	43644136	34435342	45341436
	36	51451634	64155116	55223542	15625341	32152552	53242552	32266143	11661661	26516115			
6×4×4	0	32454235	64365362	66242634	62134126	41363542	13244136	15225226	62454334	53224263	41265324	26516314	41131542
	12	55513514	53116136	32664225	64533541	22532641	41551634	43322562	11661641	66516215	41365324	62556236	41265361
	24	66114253	43244253	62264143	55223641	11435125	53324341	64365143	36642453	51661542	55645351	26326125	34363443
	36	45115135	36322561	11553614	24155215	15413514	13512634	45341435	11365163	11663641	41553416	11261542	53242552
	48	32454235	64151415	53346235	64135126	64365324	26346351	45343416	13644334	11265324	26322641	26346215	41363542
	60	62154136	15641435	15345235	64135225	66326126	13224362	26222542	13644334	26516216	41663542	32456215	62364324
	72	62132661	64133641	43114235	64153651	41665226	26622661	41535342	26224263	51153534	11555216	41663541	11553534
	84	53224226	43224341	41131463	55223426	45645334	64531561	53516352	26622662	11263542	11663542	51453415	11553416

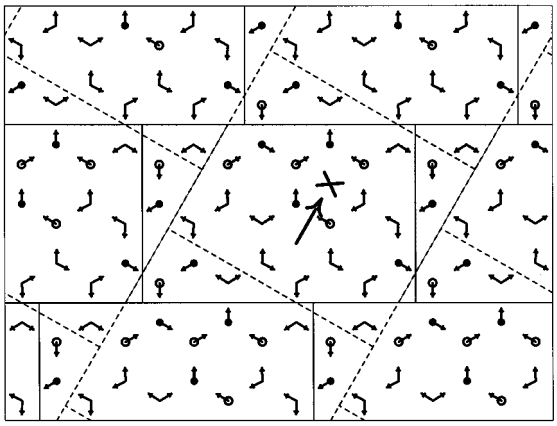

FIG. 1. Projection onto the x-y plane of one layer of Cota and Hoover's (Ref. 8) four-layer 96-molecule hexagonal ice-1h lattice; arrows indicate in-layer O–H bond vectors, while filled and open circles indicate OH bonds pointing up or down from the layer, respectively. Three equivalent representations of the lattice are indicated: (shading) hexagonal lattice, (——) $4\times1.5\times2$ pseudo-orthorhombic lattice, (- - - -) $3\times2\times2$ pseudo-orthorhombic lattice detailed in Tables III and IV with the direction of its x axis indicated.

coordination shells around a particular water molecule with OO distances $\leqslant r_{\mathrm{in}}$ is n_{in}. For each lattice so generated, the unit-cell shape is described in Table III while the orientations for the individual water molecules are specified in Table IV.

In Table II, molecules 1, 2, 5, and 6 have very similar z values, as do molecules 3, 4, 7, and 8. The ice lattice thus can be considered as comprising $2n_z$ layers stacked in the z (crystallographic c) direction. Note that oxygen sites 1 and 2 lie only in odd layers while sites 3 and 4 lie only in even layers. Each water molecule forms one hydrogen bond with a water molecule from another layer and three with waters in its own layer; a sample layer is shown in Fig. 1.

Unit cells with hexagonal hydrogen lattices can also be described efficiently in terms of our orthorhombic nomenclature. This is indicated in Fig. 1 which shows (shaded) the first of the four z layers from Cota and Hoover's 96 molecule hexagonal unit cell as it appears in the original publication,[8] as well as some additional molecules formed by replicating this unit cell in the xy plane. The hexagonal unit cell has two unique directions, and we choose one of these to be the x direction with y being perpendicular to it. Non-Bravais pseudo-orthorhombic unit cells with a bricklike stacking can then be constructed to represent the hexagonal lattice, with successive unit cells i_y (with $0\leqslant i_y<n_y$) in the y direction shifted relative to each other in the x direction by $i_y x^0_{\diagup}$. The two possible choices for the x axis give rise to two distinct pseudo-orthorhombic lattices with different periodicities, as shown in the figure using solid and dashed lines; henceforth, we adopt the representation shown in the dashed lines for which the x axis is indicated in the figure. This lattice has a $3\times2\times2$ pseudo-orthorhombic periodicity, and we use this notation to describe the 96-molecule hexagonal unit cell generated by Cota and Hoover. Use of pseudo-orthorhombic boundary conditions simplifies considerably operations using hexagonal lattices in computer simulations with (except during Ewald summations) common cubic boundary conditions requiring only trivial modification.

That the same infinite periodic ice lattice can be described in terms of a number of different unit-cell shapes and orientations has considerable implications for a unit-cell multipole expansion: different representations give rise to different multipole moments. Provided that cell boundaries are chosen so as not to pass through water molecules, the dipole moment is well behaved. In particular, if it is zero in one unit cell then it will be zero in all unit cells. The same is not true for the quadrupole and higher moments, however: converting between the hexagonal and pseudo-orthorhombic representations effects the Θ_{xy} and Θ_{xz} components of the quadrupole tensor, while rotation of the xy axes changes the diagonal components of the tensor as well. Hence, attempts to search for unit cells with zero quadrupole and octupole tensors are questionable. However, if in *any* representation the moments are zero, then the long-range electrostatic interactions (which are invariant to the cell shape) will be minimal. It is indeed the minimization of such interactions which is of importance. Note that we are unaware of any representation of Cota and Hoover's[8] cell for which the net quadrupole vanishes.

III. CRITERIA USED FOR SELECTING UNIT CELLS

A. Continuous network of hydrogen bonds

All unit cells generated are subject to the constraints that the hydrogen-bonding network is continuous, unbroken, and complete.[5,6] Each water molecule is hydrogen bonded to four neighboring water molecules.

B. Zero net dipole moment

Dipole–dipole interactions decrease in magnitude reasonably slowly and the energy of an infinite system of periodic dipoles diverges logarithmically. Hence, it is an essential property of any model ice-1h unit cell that the net dipole moment be zero. Cota and Hoover[8] showed that a simple constraint could be devised and easily implemented to allow only unit cells with zero dipole moment to be generated. We implement three alternative approaches concerning the net dipole moment. These are

(1) C0: No additional constraints; all possible unit cells are generated and later screened for zero dipole moment; this method is inefficient but can be applied to any unit cell.
(2) C1: The total number in the unit cell of each of the 24 hydrogen orientations shown in Table I is constrained to be equal; this can only be achieved if $n_x n_y n_z$ is divisible by 3.
(3) C2: The number of each of the 12 allowed hydrogen orientations per layer is constrained to be equal; this can only be achieved if $n_x n_y$ is divisible by 3.

Both constraints C1 and C2 ensure that the unit cell has zero dipole moment, with C2 introducing the further restriction that each layer individually has zero dipole moment. Cota

and Hoover's constraint, although stated differently, is equivalent to constraint C2. As shown later, this constraint is highly restrictive and may impose unwanted order on the lattice; alternatively, method C0 is computationally inefficient as a very large number of unwanted lattices are always generated. Constraint C1 provides a good compromise between computational efficiency and restrictiveness. It is a desirable constraint in its own right in that for a large random lattice, equal numbers of each possible type of water orientation are expected.

C. Zero net quadrupole moment

As discussed in Sec. II, the calculated unit-cell quadrupole moment is a function of the shape of the unit cell used to represent the infinite periodic lattice. Nevertheless, if in any shape the quadrupole moment vanishes, then long-range interactions will be minimized. We use a standardized orthorhombic (or pseudo-orthorhombic) lattice throughout, and screen the zero dipole structures for zero or small quadrupole. In general, we find that structures in which either all of the components of the quadrupole tensor vanish or all components except Θ_{xz} vanish can be found. From the structures with zero quadrupole, no structures have been found with zero octupole. We have made no attempt to isolate structures with ''low'' octupole moment as other features (see Sec. III D) are thought to be more important.

The net quadrupole moment arises from two independent contributions: from the sum of the individual water quadrupole moments, and from the spatial orientation of the water dipoles. Using either constraints C1 or C2, the contributions from the individual monomer quadrupoles vanishes. Hence, the net quadrupole moment becomes proportional to the magnitude of the dipole moment of an individual water monomer. Similarly, the net octupole moment becomes dependent only on the spatial arrangement of the water monomer dipoles and quadrupoles.

D. Randomness of hydrogen bonding

We seek hydrogen-bonding networks which are random. There are many different measures of randomness, and we consider four properties. Various ice-1h structures are then ranked on their ability to reproduce simultaneously all of these properties. If an intended use of the unit cells so generated relies heavily on a property other than those considered being random, the unit cells should be evaluated as to their appropriateness and, if necessary, revised cells generated. The properties considered herein are:

(i) The same number of each of the 24 possible hydrogen orientations is included. This is achieved automatically if constraint C1 or C2 is used.

(ii) The water dipole–dipole pair correlation function matches that for a random lattice. For coordination shell n of radius r_n, this function is defined as

$$\phi_n=\frac{\Sigma_{i=1}^{N}\Sigma_{j=1}^{i}\mathbf{a_i}\cdot\mathbf{a_j}\delta(R_{ij}-r_n)}{\Sigma_{i=1}^{N}\Sigma_{j=1}^{i}\delta(R_{ij}-r_n)}, \tag{4}$$

where R_{ij} is the distance between the nearest images of the oxygen atoms of molecules i and j. Naively, $\phi_n=0$ for no correlation (random structure) and 1 or -1 for full correlation or anticorrelation, respectively, but the constraint that the hydrogen-bonding network be continuous changes the expected values. Rahman and Stillinger[7] determined values for ϕ_n for a random continuous lattice and hence estimated the Kirkwood correlation factor

$$g_K=\sum_{n=0}^{\infty} CO_n\phi_n, \tag{5}$$

where CO_n is the shell coordination number. Note that, for shell $n=0$, $r_0=0$, $\phi_0=1$, and $CO_0=1$. We optimize structures such that the weighted sum of squares error between ϕ_n calculated for a given structure and ϕ_n as evaluated by Rahman and Stillinger is minimized. The weighting stresses the importance of the first six shells, the contribution from which dominates many important properties including the lattice energy.

(iii) The number of each possible type of in-layer nearest-neighbor interactions matches the expected value. One of the most important features we seek to establish is randomness between nearest-neighbor molecules. This is measured overall by ϕ_1, but ϕ_1 contains contributions from both nearest-neighbor interactions within one layer and between layers. For a random ensemble of water dimers in any orientation, the expected value of ϕ_1 is 1/3, but for any particular dimer, four values are possible: 1, 2/3, 0, and $-1/3$. More specifically, if the molecules are in the same layer, only values of 1 and 0 are possible while between-layer interactions can only have the values 2/3 and $-1/3$. In a lattice with N molecules, the number of (unique) interactions per molecule naively expected with values of 1, 2/3, 0, and $-1/3$ are $N/2$, $N/3$, N, and $N/6$, respectively. Rahman and Stillinger's value for ϕ_1 is 0.310 which differs from 1/3 due to constraints associated with ring formation. From our studies (see later) of clusters such as $(H_2O)_{39}$, we find that the most-important ring constraint arises from boat-type interlayer [2,2,2]-bicyclo rings. Hence, besides selecting structures on the basis of ϕ_1, we also select structures for which ratio α of the fraction of parallel in-layer nearest-neighbor overlaps with $\mathbf{a_i}\cdot\mathbf{a_j}=1$ is closest to 1/3.

(iv) The pattern of interlayer hydrogen locations matches the expected pattern for all in-layer six-membered rings. Evident in Fig. 1 are a large number ($N/2$ per unit cell) of six-membered chair-shaped in-layer rings. Every water molecule must participate in one hydrogen bond with an adjacent layer, and can be classified as one of two generic types: one that donates both of its hydrogen bonds in-layer, and one that donates one hydrogen bond in-layer and one to another layer. Each ring of water molecules can thus be classified as one of seven types depending on the ratio of the total numbers of its constituent waters of each water type which ranges from 0:6 (all molecules have a hydrogen pointing outwards) to 6:0 (all molecules have both hydrogens pointing in-layer). We select ice structures which have a random distribution β_i of these seven types of rings. Naively, probability theory using a 50%

probability for each water type can be used to determine the distribution of the various six-membered rings, but this must be modified slightly to account for hydrogen-bonding continuity. We estimate these probabilities by considering all possibilities for a water cluster $(H_2O)_6$ in its chair conformation: This approach may also be simplistic, but should provide a sufficiently reliable guide.

IV. BASIC COMPUTATIONAL PROCEDURE

The search for ice lattices (or ice clusters) is performed quite efficiently using a recursive algorithm. Once the oxygen-atom coordinates are determined [Table II, Eqs. (2) and (3)] finalizing a lattice involves simply the assignment of each water molecule to one of its six allowed hydrogen-orientation patterns from Table I. Selecting this pattern defines the local hydrogen-bonding environment for a particular water molecule. The central core of the recursive algorithm used assumes that $m(0 \leqslant m < N)$ of the N water molecules have already had orientations assigned to them; it searches for valid assignments for molecule $m+1$ by testing each of the six possible patterns in turn. A pattern is possible only if at most two hydrogen bonds are donated by and/or to both this molecule and each of its four nearest neighbors; further, it may be required to satisfy either constraint C1 or C2. For each allowable orientation, if $m+1=N$ then all waters have been assigned and a valid lattice is found, but otherwise the algorithm tentatively accepts that assignment and recurses forward, attempting to assign molecule $m+2$. Once all six possible orientations have been tried, the algorithm returns to the previous level and rejects the assignment of molecule m.

Using the above basic approach, all possible orientations in principle can be determined; in practice, however, for all realistically sized unit cells, this is not feasible directly. To overcome this we apply the basic method in various ways, and these are later described in detail: the basic method is used in some cases to generate all structures, in other cases to generate a subset of structures only, and it is also used to generate only all possible single layers of a multilayer structure. We have, however, found that the most important use of the basic algorithm is in the refinement or ''annealing'' of a known structure. This is implemented by selecting a significant number (e.g., 100–120 for large lattices or ca. $\frac{5}{6}$ of the unit cell for small ones) of connected water molecules from the structure, deleting their orientational specifications and using the basic algorithm to produce all possible replacement patterns. The water molecules to be removed can be selected in a variety of ways (e.g., slabs in the x, y, or z, etc., directions, or as spheres centred on a particular water molecule). Structures which, according to the criteria in Sec. III C, constitute an improvement then replace the old structure and the process continues until convergence. Note that, as detailed later, it is *not* recommended that the lattice potential energy be minimized during this process. Nevertheless, to facilitate escape from local minima, a generalized ''temperature'' can be introduced using a standard Monte Carlo scheme based on a generalized ''energy'' (which could be, e.g., the sum of squares error between calculated and expected lattice geometric properties *a la* Sec. III C).

Annealing provides a very efficient means for generating structures with desired properties. As starting structures for the annealing process we initially generated ones which were in themselves quite reasonable. This step proved computationally difficult, however; we found that the annealing procedure is sufficiently efficient that it is possible to use ordered starting structures. Such ordered structures could, for example, be produced by simply replicating a smaller unit cell as done by Marchi, Tse, and Klein[18] (who developed and successfully applied a complimentary annealing technique based on cycling Stillinger–Rahman loops).

V. RESULTS FOR SMALL SYSTEMS

A. Ice clusters $(H_2O)_6$ and $(H_2O)_{39}$

To estimate properties of a fully random ice lattice, two clusters are considered and all possible configurations determined. The first, $(H_2O)_6$, is a six-membered chair-type in-layer ring; for this, 730 structures are possible and the fraction of nearest neighbors with parallel dipole moments is found to be $\alpha = 0.332$; this is compared to results obtained from various ice unit cells in Table V. Also, the calculated probabilities β for six-membered rings with different numbers of all-in-layer water hydrogens are compared in Table VI.

The second cluster, $(H_2O)_{39}$, contains all molecules located in the first six coordination shells around a central molecule (this cluster actually constitutes the ''inscribed sphere'' of a 96 molecule $3\times2\times2$ lattice). It comprises three stacked layers of 13 molecules each, each layer containing three fused in-layer six-membered rings, and has overall C_{3v} oxygen symmetry. All possible hydrogen arrangements are constructed by first determining all possibilities for one layer and then all layers which can stack above or below it. Using constraint C0 (unconstrained), 400 242 patterns are possible per layer producing 8 130 532 475 772 clusters. Evaluated about the central molecule, the average values of the dipole autocorrelation functions ϕ are compared with Rahman and Stillinger's[7] values and values obtained for various lattices in Table V, as is the value obtained for α. The results for ϕ differ slightly from those of Rahman and Stillinger due to the neglect of rings of larger size. Alternatively, using constraint C2 (re-expressed so that the number included of any particular water orientation cannot exceed two per layer), the number of different layers reduces to 122 622 and the number of clusters reduces to 96 947 612 458. As shown in Table V, significant changes to the nearest neighbor and other distributions results. Hence, it is clear that Cota and Hoover's[8] constraint C2, at least when applied to lattices containing 96 of fewer molecules, on average adversely effects the randomness of the hydrogen bonding.

The results obtained here for ice-1h fragments are of course not directly relevant to the properties of real clusters of water, a field in which there is considerable historic[19–21] and current[22–24] interest. However, they do indicate the com-

TABLE V. Calculated dipole–dipole autocorrelations ϕ_n for shell n of coordination number CO_n at radius r_n (in Å at $R=2.76$ Å) for each of the selected unit cells is compared to those determined by Rahman and Stillinger (Ref. 7; R&S) and those from various ice clusters; also shown are the in-layer nearest-neighbor contribution α and the calculated Kirkwood correlation factor g_K uncorrected (Ref. 7) for the constraint of zero net dipole.

shell n	1	2	3	4	5	6	α	g_K
CO_n	4	12	1	9	6	6		
$9r_n^2/R^2$	9	24	25	33	48	49		
r_n	2.76	4.51	4.60	5.28	6.37	6.44		
R&S	f0.314	0.005	−0.095	−0.038	−0.016	0.004		1.84
$(H_2O)_{39}$	0.319	0.014	−0.084	−0.029	−0.006	0.015	0.321	
$(H_2O)_{39}$-C2	0.281	−0.033	−0.070	−0.073	0.016	0.015	0.267	
$(H_2O)_6$	0.332						0.332	
3×2×2-CH	0.250	−0.061	−0.063	−0.075	−0.058	0.007	0.250	0.22
3×2×2-h	0.302	0.008	−0.097	−0.021	0.009	0.024	0.319	2.22
3×2×2-C2	0.323	0.024	−0.104	−0.025	0.014	0.010	0.326	2.40
3×2×2-e	0.250	−0.157	0.667	−0.272	−0.148	−0.296	0.111	−4.33
3×2×2	0.312	0.012	−0.097	−0.031	−0.019	−0.016	0.333	1.81
4×3×2	0.313	0.002	−0.101	−0.044	−0.021	−0.007	0.323	1.72
4×3×2-a	0.294	−0.034	0.010	−0.078	−0.029	−0.016	0.285	1.49
5×3×3	0.314	0.001	−0.100	−0.043	−0.002	0.002	0.331	1.42
6×3×3	0.310	0.003	−0.096	−0.042	−0.020	0.009	0.327	1.33
9×5×1	0.310	0.005	−0.095	−0.038	−0.016	0.004	0.337	1.79
6×4×4	0.312	0.006	−0.102	−0.040	−0.016	0.003	0.332	1.09

plexity of such clusters, showing that an extremely large number of (marginally different) hydrogen-bonding local minima are possible.

B. Small unit cells

In addition to the six large ice-1h unit cells containing at least 96 water molecules discussed in detail in Sec. VI, 29 smaller ones are also investigated. They are relevant, as in many cases it is possible to examine all of the possible structures and thus determine unambiguously the smallest possible values for the net dipole and quadrupole moments. Hence, a more global view of the properties of ice-1h lattices can be obtained. Depending on the unit cell, we use conditions C0 (default), C1, or C2; all possible hydrogen locations are considered except for unit cells marked P (partial) for which *at least* 10^6 structures are generated. The small unit cells considered are 1×1×1, 2×1×1, 1×2×1, 1×1×2, 3×1×1, 1×3×1, 1×1×3, 4×1×1, 1×4×1, 1×1×4, 1×2×2(P), 2×1×2, 2×2×1, 5×1×1, 1×5×1(P), 1×1×5(P), 6×1×1(C1), 1×6×1(C1), 1×1×6(C1), 3×2×1(C1), 3×1×2(C1), 2×3×1(C1), 2×1×3(C1), 1×3×2(C1), 1×2×3(C1,P), 8×1×1(P), 9×1×1(C1), 3×3×1(C1), and 3×1×3(C1), while the large cells are 3×2×2(C2 and also C1, P and C0, P), 4×3×2(P), 9×5×1(P), 5×3×3(P), 6×3×3(P), and 6×4×4(P); a summary of the results obtained is:

TABLE VI. Calculated fraction β of in-layer six-membered rings with various ratios of the number of water molecules per ring with both hydrogens pointing in-layer to that with one hydrogen pointing between layers.

Cell	6:0	5:1	4:2	3:3	2:4	1:5	0:6
$(H_2O)_6$	0.003	0.058	0.247	0.386	0.247	0.058	0.003
3×2×2-CH	0.000	0.125	0.188	0.354	0.229	0.104	0.000
3×2×2-h	0.000	0.042	0.271	0.375	0.271	0.042	0.000
3×2×2-C2	0.021	0.042	0.229	0.417	0.229	0.042	0.021
3×2×2-e	0.083	0.000	0.083	0.667	0.083	0.000	0.083
3×2×2	0.000	0.063	0.271	0.333	0.271	0.063	0.000
4×3×2	0.000	0.052	0.260	0.375	0.260	0.052	0.000
4×3×2-a	0.010	0.021	0.302	0.365	0.240	0.052	0.010
5×3×3	0.000	0.056	0.256	0.383	0.244	0.061	0.000
6×3×3	0.000	0.060	0.250	0.384	0.241	0.065	0.000
9×5×1	0.000	0.056	0.256	0.378	0.256	0.056	0.000
6×4×4	0.000	0.060	0.234	0.406	0.245	0.055	0.000

(i) For the simplest 1×1×1 cell, no lattices with zero dipole exist;[2,5,13–17] we find zero dipole lattices for all 34 other unit cell dimensions considered, however.

(ii) If $n_x n_y n_z$ is divisible by 6, lattices with zero dipole and zero quadrupole exist; no lattice with zero octupole has been found, however. Note that zero dipole and quadrupole solutions can also be found in addition to those obtained using constraint C1.

(iii) If $n_x n_y n_z$ is divisible by 3 but not by 6, lattices with zero quadrupole moment are not found. Using constraint C1, lattices can always be found with all components of the traceless quadrupole tensor[25] $\boldsymbol{\Theta}$ zero except for Θ_{xz} which appears to have a minimum absolute value of

$$|\Theta_{xz}| = 8^{1/2}\mu_m R, \tag{6}$$

where μ_m is the magnitude of the water monomer dipole moment. When constraint C1 is relaxed, contributions from the water monomer quadrupole moments may also be included, but we do not find that the ''minimum'' value of the quadrupole moment could be reduced significantly through this process.

(iv) For all other unit cells, neither constraint C2 nor C1 can be applied, and the net quadrupole moment always involves summation over the individual water quadrupole tensors. Usually, a very large number of structures with a dis-

TABLE VII. Non-zero components of the net quadrupole tensor (Ref. 25) Θ in units of $8^{1/2}\mu_m R$ [see Eq. (6)] where μ_m is the water monomer dipole length and R the nearest-neighbor O–O separation [this unit is 18.3 eÅ^2 for TIP3P (Ref. 26) water at $R=2.76$ Å].

Cell	Θ_{xy}	Θ_{xz}	Θ_{yz}
3×2×2-CH	12.7	−6.0	0
3×2×2-e	8.5	0	−20.8
4×3×2-a	−4.2	−4.0	−3.5
5×3×3	0	1	0
9×5×1	0	1	0

TABLE IX. Classical energy, in kcal mol^{-1} for the selected unit cells obtained using the TIP3P (Ref. 26), SPC/E (Ref. 27) and RWK2 (Ref. 28) pair potentials at their respective intramolecular geometries and $R=2.76$ Å; the observed (Ref. 29) infinite-lattice value is $U=-14.08$ kcal mol^{-1}.

Cell	TIP3P	SPC/E	RWK2
3×2×2-CH	−15.391	−14.319	−13.559
3×2×2-h	−15.080	−14.000	−13.346
3×2×2-C2	−15.065	−13.990	−13.333
3×2×2	−15.094	−14.018	−13.358
3×2×2-e	−16.338	−15.277	−14.185
4×3×2	−15.270	−14.224	−13.527
4×3×2-a	−15.281	−14.232	−13.532
5×3×3	−15.396	−14.425	−13.725
6×3×3	−15.392	−14.420	−13.722
9×5×1	−15.069	−13.994	−13.354
6×4×4	−15.420	−14.463	−13.761

tribution of quadrupole tensor elements quite close to zero (e.g., less than the value for a water monomer) can be found, although we find none for which all elements are precisely zero.

VI. RESULTS FOR LARGE UNIT CELLS

For each of the six large unit-cell shapes (A–F) discussed below, a single fully optimized lattice has been selected and its structure is given in Table IV; some other pertinent structures are also included therein. For all of these lattices, basic lattice properties appear in Table III, calculated pair correlations ϕ_i (for $i=1\rightarrow 6$), α, and g_K appear in Table V, ring analyses β in Table VI, lowest nonzero multipole moments in Tables VII (quadrupole) or VIII (octupole), and lattice energies evaluated using an assortment of pair-potential functions commonly used in different contexts (TIP3P,[26] SPC/E,[27] and RWK2[28]) appear in Table IX. Figure 2 also shows ϕ for those unit cells with more than six coordination shells.

From the data given in Tables I–IV using Eqs. (1) and (2), it is possible to generate the complete Cartesian coordinates for the ice lattices.[29] For lattices with $R_{OH}=0.9572$ Å, $\theta=104.5°$, and $R=2.76$ Å such Cartesian coordinates are provided for all lattices in Supplementary Data;[30] note, however, that when these lattices are used in conjunction with specific water–water potential surfaces, other values of these geometric parameters may be appropriate.

A. 3×2×2 (96 molecules)

This is the larger of the unit cells considered originally by Cota and Hoover;[8] a layer from their structure is shown in Fig. 1, while Tables III–IX show numerical results for their lattice under the name ''3×2×2-CH.'' Making use of vastly increased computational resources, we have repeated their (1977) calculation considering all possible structures obtained using condition C2; this facilitates an informed choice of a representative single lattice. We also consider both hexagonal and orthorhombic lattices: qualitatively, the results for the two different lattice symmetries are very similar, and we describe in detail those for orthorhombic symmetry only.

A total of 53 544 hydrogen-bonding arrangements are possible for each of the four layers in the unit cell, but of these only 2276 configurations are unique, the other configurations being generated by application of the oxygen-lattice crystallographic translation, rotation, and inversion symmetry operators. These layers may be stacked both above and below each other in pairs, each in a grand total of 1 598 904 ways. Viable 96-molecule unit cells are then formed by starting with one of the 2276 unique layers and stacking three additional layers on top. A total of 7 312 420 unique ice-1h unit cells are thus generated, with a grand total of 643 669 008 unit cells possible. Note, however, that of the unique unit cells, only about half of these have unique atomic pair correlation functions (and thus produce different energies using a pairwise-additive intermolecular potential function). Of the unique unit cells, 35 965 are found to have zero quadrupole moment; the total number of such cells is 3 214 896 or just 0.5% of the total. No unit cells have zero octupole moment.

One feature which is immediately apparent is the dramatic *reduction* by a factor of 150 in the number of possible

TABLE VIII. Components of the net octupole tensor (Ref. 25) Ω for unit cells with zero net quadrupole, in eÅ^3, evaluated using TIP3P (Ref. 26) water ($\mu_m=2.347$ D) at $R=2.76$ Å.

Cell	Ω_{xxx}	Ω_{yxx}	Ω_{yyx}	Ω_{yyy}	Ω_{zxx}	Ω_{zyx}	Ω_{zyy}	Ω_{zzx}	Ω_{zzy}	Ω_{zzz}
3×2×2-h	−380	0	500	0	−170	−50	80	−120	0	90
3×2×2-C2	0	70	0	190	−470	150	−150	0	−260	610
3×2×2	170	0	60	10	−10	50	40	−230	0	−30
4×3×2	−30	860	420	−640	730	1030	70	−380	−220	−800
6×3×3	290	510	730	−390	−1060	1120	140	−1020	−120	930
6×4×4	−340	−1400	−130	1560	−4630	−1990	1150	460	−170	3480

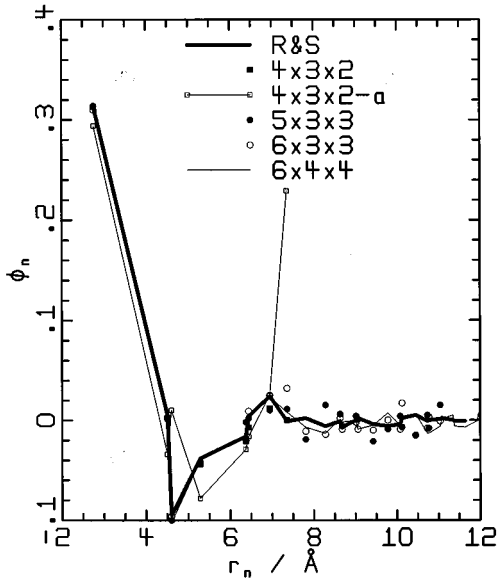

FIG. 2. Plot of the dipole–dipole autocorrelation function ϕ for various shells as a function of the shell radius at $R=2.76$ Å, as well as the results of Rahman and Stillinger (Ref. 7; R&S).

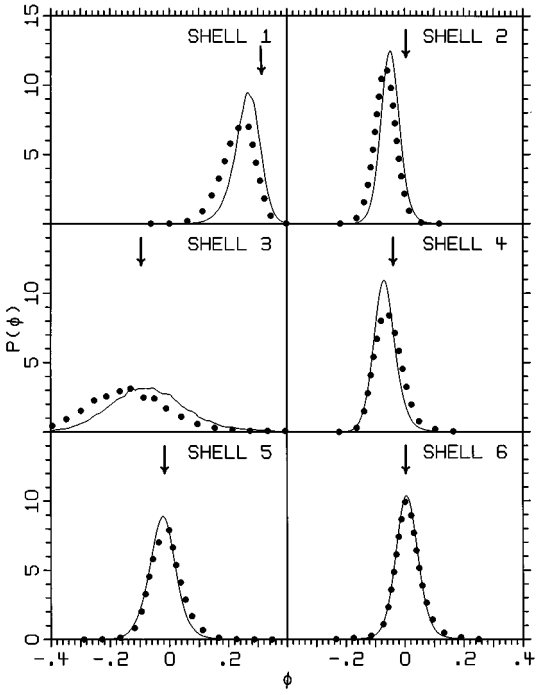

FIG. 3. Probability of occurrence for $3\times2\times2$ unit cells under condition C2 of the hydrogen-bonding autocorrelation functions ϕ for water molecules in various coordination shells (see Table V): (——) full configuration space, (●) zero quadrupolar configurations only; (↓) Rahman and Stillinger's (Ref. 7) results for a random lattice.

structures from the cluster $(H_2O)_{39}$ to the zero dipole infinitely periodic 96-molecule unit cell. Clearly, the imposed restrictions have a large impact on the available configuration space. For larger unit cells, the effects of the boundary conditions will diminish and hence the number of possible structures increases extremely rapidly for small size increases, suggesting that the generation of any complete set of lattices containing more than 96 molecules is unlikely. Indeed, different approaches are taken for the larger cells considered below.

From all possible unit cells, properties of the one which optimizes the conditions described in Sec. III are shown in Tables III–IX as cell ''$3\times2\times2$-C2''; the analogous structure obtained using hexagonal symmetry is therein named ''$3\times2\times2$-h.'' These structures do not differ significantly among themselves, and based on our criteria, both are significant improvements over the original Cota and Hoover cell. Using the annealing algorithm, structure $3\times2\times2$-C2 was reoptimized using constraint C1, and properties of the resulting unit cell, named simply ''$3\times2\times2$,'' are also shown in the tables. This relaxation improves the pair correlation shown in Table V somewhat, but has only a small effect on the calculated pair correlation energies shown in Table IX.

We have also considered the range of properties available to unit cells using condition C2: Fig. 3 shows the probability of occurrence of unit cells with different values of ϕ, Fig. 4 shows the probability of different RWK2 classical lattice energies, and Fig. 5 shows the correlation of this lattice energy with ϕ_1. Results are shown for both the full unit-cell set and the set with zero quadrupole. Quite larger variations are seen in the pair correlation functions, especially for the nearest-neighbor interactions which dominate the unit-cell energy. The broadest distribution is for ϕ_3, the infrequent interlayer interaction between the apexes of the [2,2,2]-bicyclo rings. For many of the functions considered, the random ice results lie near the *tail* of the distribution, an expected result given the large distortion in the structure of $(H_2O)_{39}$ shown in Table V as a result of imposition of constraint C2. Thus only ca. 1 in 10^6 of the zero dipole unit cells are, according to our criteria, found to be qualitatively reasonable; clearly one must be very careful in choosing unit cells for ice-1h. Similar large variations are also found for other properties such as α and β. Results (not shown) for the SPC/E and TIP3P potentials are directly analogous to those shown in Figs. 4 and 5 for the RWK2 potential; for each

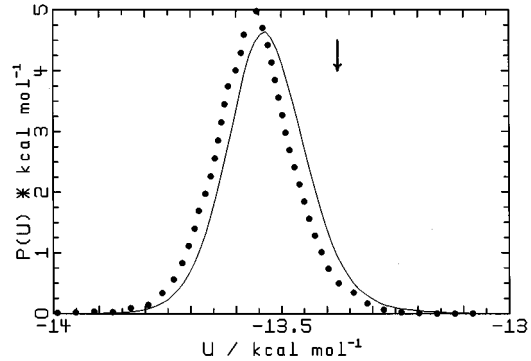

FIG. 4. Probability of occurrence for $3\times2\times2$ unit cells under condition C2 of the RWK2 classical average lattice energy (at $R=2.76$ Å) per molecule, U: (——) full configuration space, (●) zero quadrupolar configurations only, (↓) the energy of the selected configuration named ''$3\times2\times2$-C2.''

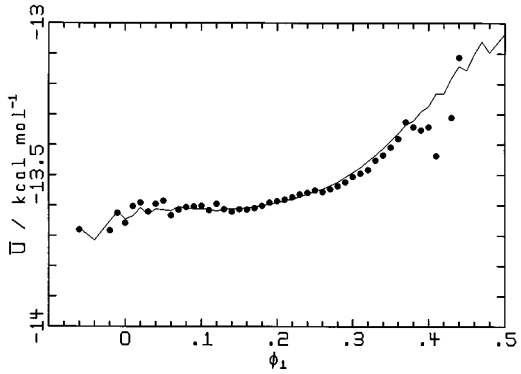

FIG. 5. RWK2 lattice energy at $R=2.76$ Å, averaged over regions of width $\Delta\phi_1=0.01$ for $3\times2\times2$ lattices under condition C2 as a function of the nearest-neighbor hydrogen-bonding correlation ϕ_1: (——) full configuration space, (●) zero quadrupolar configurations only. Note that poor sampling occurs for extremum ϕ_1.

potential, a total energy spread of ca. 1 kcal mol^{-1} is found, of the same order as the differences in energies between potentials shown for the same configuration in Table IX. Hence, when comparing results obtained using different models, it is essential either that the same ice structure is used or that, if different structures are required, then these structures must be internally consistent.

It is possible (see, e.g., Ref. 12) to optimize unit cells for ice-1h by minimizing the lattice energy. From our complete set of lattices obeying constraint C2, we find that one structure is actually the lowest energy structure for *all* three potentials considered; properties of this lattice, named ''$3\times2\times2$-e,'' are also described in the results tables and figures. Note, however, that this lattice actually comprises two units of a smaller $3\times2\times1$ lattice. It is highly ordered with very strong pair correlations (see Table V; also, *all* interlayer nearest-neighbor interactions have $\phi_1=2/3$) and regular six-membered rings (see Table VI); it is clearly not a representative structure for ice-1h. While free-energy minimizations on large samples should give reasonable results, potential-energy minimizations on small samples may not.

B. 6×3×3 (432 molecules)

Due to the increased sample size, it is not possible to generate all unit cells, even using condition C2. As reasonably random structures for the $3\times2\times2$ lattice are found to be rather infrequent, an algorithm for constructing a $6\times3\times3$ cell was developed biased towards the generation of random structures with zero quadrupole. The 432 interlayer hydrogens were targeted, and their positions determined first. A stochastic algorithm was used, placing the hydrogens subject to the β constraint and a constraint necessary to obtain zero quadrupole (in every xz and yz plane of the cell, an equal number of OH vectors are set pointing towards $+z$ and $-z$). All possible in-layer patterns are then generated with the chosen between-layer hydrogens. Unfortunately, the chance of finding *any* solution for a particular layer in these circumstances is small, and all six layers must be independently matched in order to obtain a valid ice lattice. If a solution exists for a layer, then usually 10–100 different solutions also exist, and the first (of ca. 10^7) interlayer pattern to be successfully matched produced 10^6 zero quadrupole unit cells! From this set we selected and annealed one unit cell and its properties are shown in Tables III–IX and Fig. 2. Clearly, this lattice satisfies all of the selection criteria.

C. 5×3×3 (360 molecules)

As indicated in Table II, this lattice is important as it is close to being cubic (the next largest unit cell with a higher ratio of its inscribed volume to its total volume is $14\times8\times9$). The algorithm used for the $6\times3\times3$ cell requires n_xn_z to be even and so cannot be applied here. Instead, we chose first a set of 300 individual layers as described in Sec. VI A, additionally requiring them to have random six-membered rings and intralayer pair correlations. These are then placed on odd layers in the lattice and all possible even layers determined, producing 10^5 unit cells; one is then chosen and annealed, the annealing removing any trace of the differing histories of the odd and even layers. In all, over 10^7 unit cells were examined of which 5×10^4 displayed the (apparent) minimum value given by Eq. (6). From Tables III–IX and Fig. 2, it is clear that the finally selected unit cell satisfies all of the randomness criteria.

D. 4×3×2 (192 molecules)

A unit cell of this dimension has been generated by Deutsch *et al.*,[9] and we show its properties under the name ''$4\times3\times3$-a'' in Tables III–IX and Fig. 2. While no serious deficiencies are apparent, room for improvement is seen. We annealed it, producing the unit cell named ''$4\times3\times2$'' in the results tables and figures. This structure again clearly meets all of our selection criteria.

E. 9×5×1 (360 molecules)

This lattice forms a thin slab and contains four nearly square ice-1h surfaces. It has been optimized using the same criteria as the other lattices, but six coordination shells are included in the optimization even though this exceeds that actually contained within the inscribed volume. The results shown in Tables III–IX indicate that our selection scheme can also be applied to construct model ice-1h surfaces that are internally consistent with more extensive models for bulk ice. It is easily applied to generate structures for any desired crystal face, and could be modified to allow for surface reconstruction effects.

F. 6×4×4 (768 molecules)

This unit cell is obtained by annealing a structure generated simply as eight copies of the $3\times2\times2$ unit cell. During the annealing process, 55% of water molecules changed orientation, and 343 of the 384 six-membered rings were altered; of the eight original copies of each of the 48 six-membered rings of the $3\times2\times2$ lattice, only for two rings

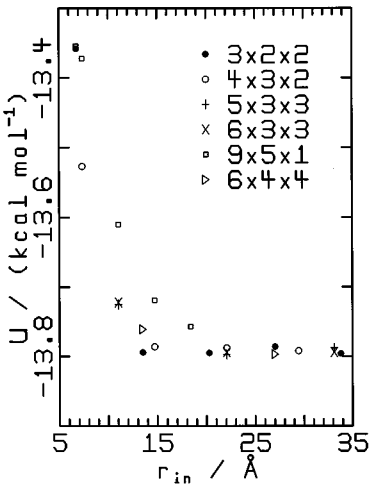

FIG. 6. RWK2 classical lattice energy U for large ice-1h lattices at $R=2.76$ Å obtained by replicating the basic unit cell 1–5 times in each direction, shown as a function of the inscribed radius r_{in} of the enlarged unit cell; the observed (Ref. 29) value is $U=-14.08$ kcal mol^{-1}.

did at most duplicate copies remain intact. Hence, the final product is thought to be significantly different from the original, and its energy shown in Fig. 6 is closer to the infinite-sample limit (see later) than that of the simply replicated original. Perhaps the most significant effect of the annealing is a reduction by a factor of 20 of the root-mean-square deviations for the long-range correlations $\phi_7-\phi_{36}$; the absence of significant long-range correlation for the final structure is evident in Fig. 2. This lattice may be cut in a number of ways to produce sizeable representations of various ice-1h surfaces.

VII. LONG-RANGE INTERACTIONS

The drive to obtain unit cells with small multipole moments arises as one wishes to minimize long-range electrostatic interactions between unit cells. If in any representation of an infinite structure the net quadrupole moment is zero, then these interactions will be minimized, but nonuniqueness of the quadrupole moment makes this principle difficult to apply. Using the RWK2 potential we have calculated the effects of long-range interactions on the average internal energy U, and the results are shown in Fig. 6. The large unit cells considered in Sec. VI are taken and replicated in real space forming larger cells, and U is shown as a function of the inscribed radius of the enlarged cell. All interactions are included in the energy, although the dispersion and Coulomb terms[28] dominate the lattice sums. U falls by ca. 0.35 kcal mol^{-1} as the cell size expands from 96 to 360 molecules and a further ca. 0.07 kcal mol^{-1} to convergence at ca. 3000 molecules ($r_{\text{in}}\approx 20$ Å). The most interesting feature of Fig. 6 is that, averaged over all six expanded lattices with $r_{\text{in}}>20$ Å, the infinite lattice energy converges to -13.793 ± 0.004 kcal mol^{-1} whereas the standard deviation of the complete set of C2 constrained $3\times2\times2$ unit cells from Fig. 4 is 0.094 kcal mol^{-1} and the overall energy range exceeds 1 kcal mol^{-1}. Hence, the various ice lattices including the $9\times5\times1$ slab, although of considerably varying shape and development history, are highly self-consistent.

There is no distinction detectable between the long-range behavior of our $6\times3\times3$ unit cell which has ''zero quadrupole'' and our $5\times3\times3$ unit cell, which does not. Indeed, this may arise as the important interactions appear to be of a length scale smaller than the radius of convergence of the multipole expansion. We also investigated the long-range properties of an additional 96-molecule unit cell selected from our complete set of C2 unit cells using the criterion that the sum of the absolute value of the elements of the quadrupole tensor is maximized. Its RWK2 lattice energy decreases from -13.3 kcal mol^{-1} to (a converged value of) -13.8 kcal mol^{-1} as r_{in} increased from 6.76 to 20 Å, directly analogous to the results for the (zero quadrupole) $3\times2\times2$ lattice shown in Fig. 6. This also suggests that quadrupole–quadrupole interactions do not contribute significantly to the long-range interaction energy.

VIII. CONCLUSIONS

While lattices that have previously been used for the simulation of ice-1h have usually been adequate for their intended purpose, we present a method for the generation of consistent, improved structures with quantified hydrogen-bonding randomness. It is applied herein to generate model unit cells containing 96, 192, 360, 432, and 768 water molecules intended to model both ice-1h bulk and surfaces. Other unit cells could be generated for specific purposes, but the *internal consistency* seen between lattices implies that, for a specifically generated lattice, properties that are not dependent on the actual dimensions will change only slightly; arbitrarily chosen lattices can, in principle, display large variations in such properties. Our method may easily be modified to create alternate sets of unit cells optimized using additional or alternate constraints (e.g., for the three-body correlation functions), if warranted.

Most methods used for generating ice-1h lattices have relied on the constraint (C2) of Cota and Hoover[8] which ensures that unit cells have zero net dipole moment. We find that this constraint is too restrictive, however, and implement an alternate weaker constraint (C1). Especially for smaller unit cells containing 96 or less molecules, their constraint severely limits the randomness of the hydrogen bonding attainable. For the $6\times3\times3$ and $5\times3\times3$ lattices, we applied a considerable number of ''intelligent'' schemes designed to produce lattices which simultaneously fulfilled multiple selection criteria. We found this process to be time consuming and unproductive, and support other recommendations[18] for the use of simplistic annealing schemes based on crude starting structures. Note, however, that use of potential-energy-minimization techniques to obtain ice-1h structures[12] could easily produce unrealistic, highly ordered structures and is not recommended.

ACKNOWLEDGMENTS

Support for this work from the Australian Research Council (A 29530010 and F29600328) is gratefully acknowledged. We thank Professor A. D. J. Haymet for raising these matters and for helpful comments.

[1] M. Matsumoto and Y. Kataoka, J. Chem. Phys. **88**, 3233 (1988).
[2] O. A. Karim and A. D. J. Haymet, J. Chem. Phys. **89**, 6889 (1988).
[3] G.-J. Kroes, Surf. Sci. **275**, 365 (1992).
[4] H. Nada and Y. Furukawa, Jpn. J. Appl. Phys. **34**, 583 (1995).
[5] J. D. Bernal and R. H. Fowler, J. Chem. Phys. **1**, 515 (1933).
[6] W. F. Kuhs and M. S. Lehmann, in *Water Science Reviews 2*, edited by F. Franks (Cambridge University Press, Cambridge, 1986).
[7] A. Rahman and F. H. Stillinger, J. Chem. Phys. **57**, 4009 (1972).
[8] E. Cota and W. G. Hoover, J. Chem. Phys. **67**, 3839 (1977).
[9] P. W. Deutsch, B. N. Hale, R. C. Ward, and D. A. Reago Jr., J. Chem. Phys. **78**, 5103 (1983).
[10] R. E. Kozack and P. C. Jordan, J. Chem. Phys. **96**, 3120 (1992).
[11] A. D. J. Haymet (private communication).
[12] H. Gai, G. K. Schenter, and B. C. Garrett, J. Chem. Phys. **104**, 680 (1996).
[13] K. Smimaoka, J. Phys. Soc. Jpn. **15**, 106 (1960).
[14] M. D. Morse and S. A. Rice, J. Chem. Phys. **76**, 650 (1982).
[15] B. J. Yoon, K. Morokuma, and E. R. Davidson, J. Chem. Phys. **83**, 1223 (1983).
[16] E. R. Davidson and K. Morokuma, J. Chem. Phys. **81**, 3741 (1984).
[17] A. J. Leadbetter, R. C. Ward, J. W. Clark, P. A. Tucker, T. Matsuo, and H. Suga, J. Chem. Phys. **82**, 424 (1985).
[18] M. Marchi, J. S. Tse, and M. L. Klein, J. Chem. Phys. **85**, 2414 (1986).
[19] J. R. Reimers and R. O. Watts, Chem. Phys. **85**, 83 (1984).
[20] D. F. Coker, R. E. Miller, and R. O. Watts, J. Chem. Phys. **82**, 3554 (1985).
[21] R. H. Page, J. G. Frey, Y. R. Shen, and Y. T. Lee, Chem. Phys. Lett. **106**, 373 (1984).
[22] C. Lee, H. Chen, and G. Fitzgerald, J. Chem. Phys. **102**, 1266 (1995).
[23] S. S. Xantheas, J. Chem. Phys. **102**, 4505 (1995).
[24] A. Khan, Chem. Phys. Lett. **253**, 299 (1996).
[25] A. D. Buckingham, Quart. Rev. **13**, 193 (1959).
[26] W. L. Jorgensen, J. Chandrasekhar, J. D. Madura, R. W. Impey, and M. L. Klein, J. Chem. Phys. **79**, 926 (1983).
[27] H. J. C. Berendsen, J. R. Grigera, and T. P. Straatsma, J. Phys. Chem. **91**, 6269 (1987).
[28] J. R. Reimers, R. O. Watts, and M. L. Klein, Chem. Phys. **64**, 95 (1982).
[29] E. Whalley, in *Physics and Chemistry of Ice*, edited by E. Whalley, S. J. Jones, and L. W. Gold (Royal Society of Canada, Ottawa, 1993).
[30] See AIP Document No. E-PAPS: E-JCPSA-106-1518 for 1 file of coordinates of ice-1h lattices which has been filed electronically in ASCII. E-PAPS document files may be retrieved free of charge from our FTP server (http://www.aip.org/epaps/epaps.html). For further information: e-mail: paps@aip.org or fax: 516-576-2223.